An Empirical Approach to Omnidirectional Path Loss and Line-of-sight Probability Models at 18 GHz for 5G Networks

N. O. Oyie and T. J. O. Afullo
Discipline of Electrical, Electronic and Computer Engineering
University of KwaZulu-Natal, Durban 4041, South Africa

Abstract— Millimeter wave frequency bands present a huge bandwidth for fifth generation wireless communication networks. Wireless networks deployment within indoor environments will pose a challenge due to propagation characteristics of signals at millimeter wave frequency bands. This paper presents an empirical analysis of the impact of a building's structural and material design on omnidirectional path loss and line-of-sight probability models in indoor environments. Path loss and line-of-sight probability are important aspects of indoor propagation characteristics as they determine overall network coverage capacity. The studied models address the deficiencies of the current models in terms of accuracy and reliability. The models are synthesized from measurements conducted at 18 GHz frequency band on the 5th floor of the Discipline of Electrical, Electronic and Computer Engineering building, University of KwaZulu-Natal, Durban, South Africa. A costume-designed channel sounder based on Rohde and Schwarz SMF 100 A signal generator and FSIQ 40 signal analyzer with 120 MHz bandwidth was used. More than 13 unique transmitter-receiver combinations were considered in a distance range of 2 m to 24 m. The acquired measurement data was post-processed and an omnidirectional dual-slope path loss and improved line-of-sight probability model was developed and fitted on it using minimum root mean square technique. The applications of these models were supported by detailed consideration and analysis of propagation mechanisms in an indoor corridor such as reflection and diffraction, resulting in modal propagation. The models were evaluated by comparing the simulated omnidirectional dual-slope path loss and improved line-of-sight probability model with the corresponding measurements and existing models. The results were observed to compare well with the well-known path loss close-in reference model and existing line-of-sight probability models.

1. INTRODUCTION

Higher data rates are demanded for future applications in the fifth generation (5G) wireless communication systems. Millimeter wave band promises a huge bandwidth that can deliver multi-gigabit communication services required for 5G applications [1, 2]. The characterization and modeling of millimeter wave propagation in indoor corridor environments are some of the most important steps in developing 5G mobile access networks. The current focus of research in the study of propagation characteristics, channel modeling, beamforming, and access control is related to millimeter wave communications [1]. The electronically-steerable adaptive antennas will be used in 5G millimeter wave communication systems [3–5], however, many reseachers are using mechanically rotatable horn antennas for measurements at millimeter wave frequency bands [3, 6, 7]. Omnidirectional antennas require much greater transmit power compared to directional antennas to achieve the same maximum measurable range.

The omnidirectional antenna pattern synthesis was applied to generate omnidirectional path loss models at 18 GHz using directional measurements [8]. This was achieved by summing up the received power at each and every unique measured non-overlapping transmit and receive antenna pointing angle combination. In addition, with the transmitter (Tx) and receiver (Rx) antenna gains removed from the directional measurement, the omnidirectional path loss was determined by subtracting the summed received power [3].

In this paper, an empirical approach to omnidirectional path loss model is presented. This paper further proposes a line-of-sight (LOS) probability model for indoor corridors at 18 GHz frequency band. The synthesized omnidirectional antenna pattern is validated by omnidirectional received power from all the measured uniques pointing angles. The transmit and receive antennas are rotated over azimuth and elevation planes. This approach reaps benefits of directional gain while applies the synthesized omnidirectional antenna pattern to model the omnidirectional path loss. For effective design of wireless communication systems, path loss models are required in estimation of the attenuation of signal power over distance [3]. It is essential for indoor corridor environments to have accurate path loss models for applications in the future generation communication systems.

This paper compares two empirical path loss models i.e., the dual slope (DS) and the close-in (CI) free space reference distance models.

LOS probability has been investigated based on millimeter wave propagation in indoor corridors. The network coverage capability for 5G radio access systems will depend on the LOS probability in indoor corridor propagation. The LOS probability models so far applied in system level evaluation activities are less suitable due to changes in the requirements for 5G network indoor deployments [9–11]. Consequently, a new LOS probability model is introduced in this paper to improve the accuracy and facilitate the evaluation work for 5G technologies and solve the deficiency of the existing models (see Table 2). The proposed model is validated by 18 GHz indoor corridor measurements and compared with existing models.

The rest of this paper is organized as follows: measurement setup is described in Section 2. In Section 3, synthesis of the omnidirectional path loss is presented while Sections 4 provides the measurement and simulations of the horn antenna radiation pattern. Sections 5 and 6, present DS and CI path loss models. Section 7 presents the results and discussions. Finally, this paper is concluded in Section 8.

2. MEASUREMENT SETUP

Figure 1 shows the floor plan and description of the measurement environment. The 18 GHz measurements were performed within indoor corridors of the 5th of the Discipline of Electrical, Electronic and Computer Engineering building, University of Kwa-Zulu Natal, South Africa. The corridor dimensions are 1.4 m × 24 m and the ceiling height is 2.7 m. The environment is a typical indoor corridor, a waveguide like structure with walls made of bricks and dry concrete, tiled floor and plasterboard on ceiling, wooden doors to offices, a staircase and an elevator [8]. The channel sounder was based on Rohde and Schwarz SMF 100 A for radio frequency signal generation at the Tx side with a frequency range of 100 kHz to 22 GHz while Rx equipment was Rohde and Schwarz FSIQ 40 Signal Analyzer with a frequency range of 20 Hz to 40 GHz and maximum analysis bandwidth of 120 MHz. Measurement system consisted of a pair of wideband vertically polarized (V-V) directional pyramidal horn antennas with a 20.95 dBi gain, 3 dB beamwidth of 15.6° in elevation and 15.4° in azimuth at 18 GHz. As depicted in Fig. 1, the Tx system was stationary while Rx system was moved along the corridor in steps of 2 m from each and every measurement point. A continuous wave was transmitted by the transmitter at 10 dBm and received power recorded at the receiver [8].

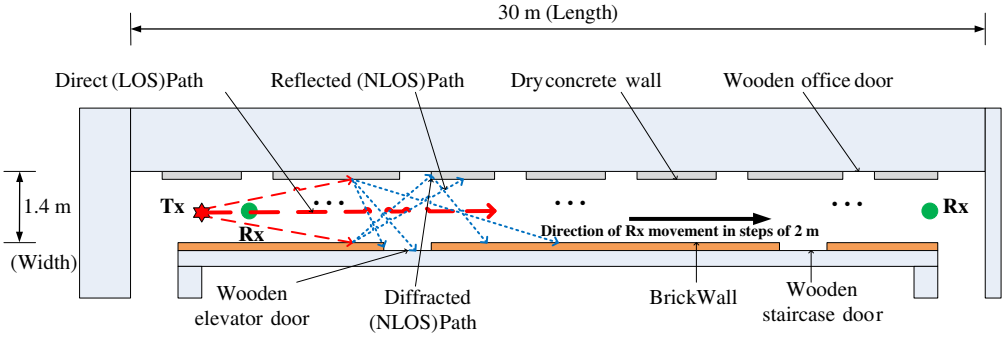

Figure 1: Floor plan of the indoor corridor.

The horn antenna radiation pattern was measured in an anechoic chamber for the azimuth and elevation patterns with a V-V polarization of the antennas. The Rx antenna was rotated in steps of 2.5° in the azimuth plane (360°) and elevation plane (−90° and 90°).

3. OMNIDIRECTIONAL PATH LOSS SYNTHESIS

Omnidirectional LOS path loss was established in the corridor for scenarios where Tx and Rx had no obstruction between them and pointed at each other with alignment on boresight for each exclusive antenna pointing angles in every Tx and Rx combination [8, 15].

The omnidirectional path loss was determined by subtracting the summed received power from the transmit power, with the Tx and Rx antenna gains removed from each directional measurement

and can be expressed as [3].

$$PL_{i,j}[\mathrm{dB}] = Pt_{i,j}[\mathrm{dB}] - 10\log_{10}\left(\sum_{n}\sum_{m}\sum_{l}\sum_{k} Pr_{i,j}(\phi_k, \theta_l, \varphi_m, \vartheta_n)[\mathrm{mW}]\right) \tag{1}$$

where $PL_{i,j}$, $Pt_{i,j}$, and $Pr_{i,j}$ denote the synthesized omnidirectional path loss, synthesized omnidirectional transmit power, and directional received power for a specific and unique angle of departure (AOD) and angle of arrival (AOA) combination (with the antenna gains removed) from the ith Tx to the jth Rx, respectively. ϕ, θ, φ, ϑ are the azimuth AOA, elevation AOA, azimuth AOD, and elevation AOD, respectively [3].

4. HORN ANTENNA RADIATION PATTERN

The antenna radiation pattern can be used to validate the synthesized omnidirectional received power. The power radition pattern of a horn antenna can be approximated by [12]:

$$f(\phi,\theta) = G[\mathrm{sinc}^2(\mathrm{a}\cdot\sin(\phi))\cos^2(\phi)]\cdot[\mathrm{sinc}^2(\mathrm{b}\cdot\sin(\theta))\cos^2(\theta)] \tag{2}$$

where ϕ and θ represent the azimuth and elevation angles with respect (w.r.t) the antenna boresight, respectively. $f(\phi,\theta)$ denotes the radiation power density at ϕ and θ, G represents the boresight gain of the antenna. a and b are functions of the azimuth (AZ) and elevation (EL) half power beamwidth (HPBW) of the horn antenna, respectively such that [3, 12]:

$$\mathrm{sinc}^2\left(\mathrm{a}\cdot\sin\left(\frac{HPBW_{AZ}}{2}\right)\right)\cos^2\left(\frac{HPBW_{AZ}}{2}\right) = \frac{1}{2} \tag{3}$$

$$\mathrm{sinc}^2\left(\mathrm{b}\cdot\sin\left(\frac{HPBW_{EL}}{2}\right)\right)\cos^2\left(\frac{HPBW_{EL}}{2}\right) = \frac{1}{2} \tag{4}$$

The normalized antenna azimuth power pattern (simulated and measured) with an azimuth HPBW of 15.4° at an elevation angle of 0° and at azimuth angles of 0° and 15.4° and −15.4° w.r.t boresight angle are displayed in Figs. 2(a), 2(b) and 3(a), respectively, while normalized equivalent widebeam antenna power pattern by linear combination of the power amplitude of each adjacent azimuth angles is displayed in Fig. 3(b). The maximum gain in the normalized equivalent pattern remains constant over the range −15.4° to 15.4°. This shows that by summing up the power patterns at antenna pointing angles over the entire azimuth plane (0° to 360°), the resultant antenna gain will become constant over the entire azimuth plane and approximately equal to the boresight gain of the directional horn antenna. The same result holds for the elevation plane. When this same concept is

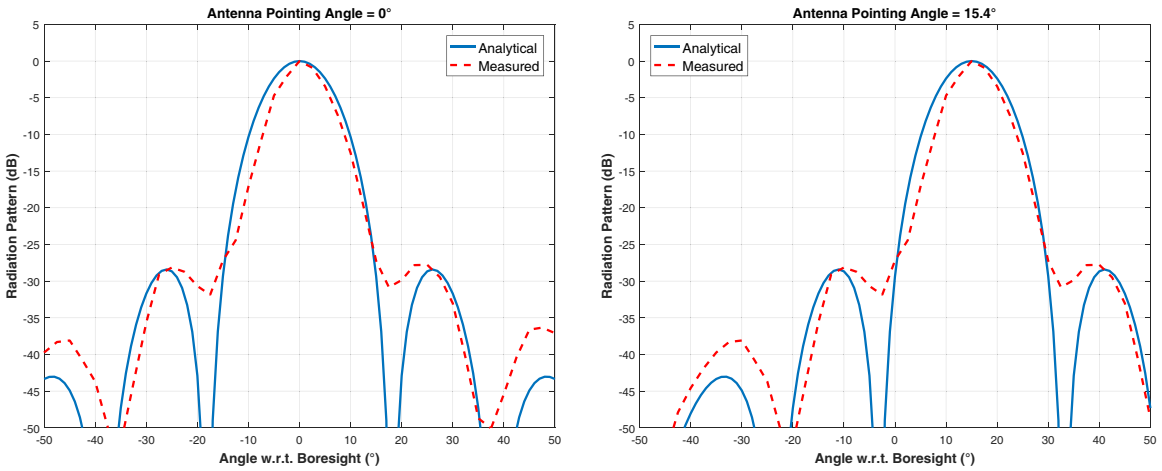

(a) (b)

Figure 2: Normalized antenna pattern in the azimuth plane for a horn antenna with an azimuth HPBW of 15.4° at 0° and 15.4° azimuth pointing angles w.r.t. the boresight angle. (a) Antenna pointing angle at 0°. (b) Antenna pointing angle at 15.4°.

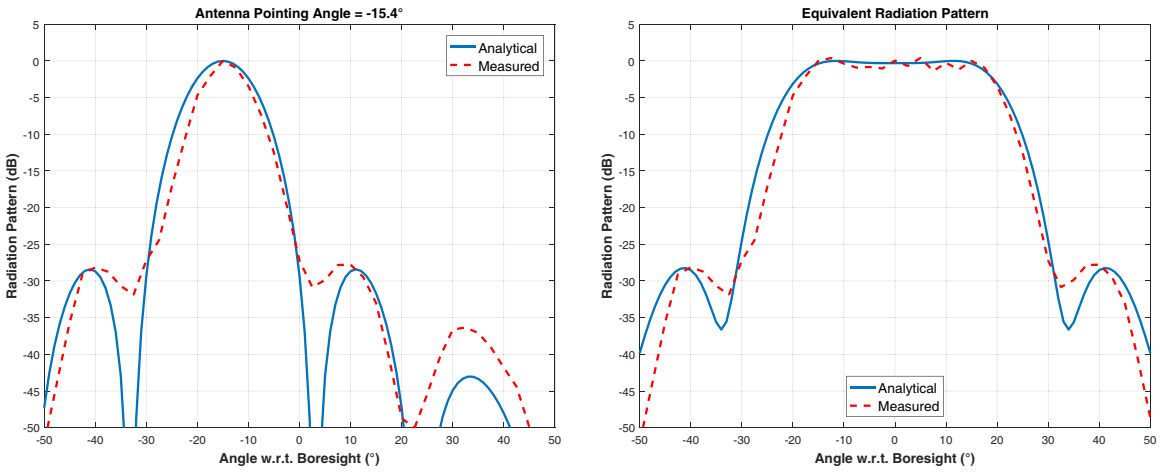

(a) (b)

Figure 3: Normalized antenna pattern in the azimuth plane for a horn antenna with an azimuth HPBW of 15.4° at −15.4° azimuth pointing angles w.r.t. the boresight angle and the equivalent radiation pattern for 0° 15.4° and −15.4° anlges. (a) Antenna pointing angle at −15.4°. (b) Equivalent radiation pattern.

extracted over the entire 4π steradian sphere, the synthesized directional horn antenna pattern after removing the gain approximates omnidirectional antenna pattern. This clearly demonstrates that it is appropriate to generate the omnidirectional received power by linearly combining the powers from directional antennas in all possible non-overalpping directions, with antenna gain removed as provided in (1).

5. DUAL SLOPE PATH LOSS MODEL

The possible modes in a rectangular waveguide i.e., (m, n) modes can be geometrically described as a cluster of propagating wave into the corridor reflected on the vertical and horizontal walls with proper grazing angles $\phi_V^{m,n}$ and $\phi_H^{m,n}$ respectively. The electromagnetic field produced by these waves propagate progressively along the corridor's axis and on the contrary a full standing wave in the xy plane, where the waves superimpose to produce the (m, n) mode behavior [13].

The modal attenuation factor (MAF) value, denoted by $L_{m,n}$[dB], is given in Eq. (5). MAF is the power loss due to the multiple reflections on the mode wavefronts on the corridor walls and can be expressed as [13]:

$$\begin{aligned} L_{m,n}[\text{dB}] &= 10\left(N_V^{m,n}\cdot\log_{10}\frac{1}{|R_V(\phi_V^{m,n})|^2}+N_H^{m,n}\cdot\log_{10}\frac{1}{|R_H(\phi_H^{m,n})|^2}\right) \\ &= 10d\left(\frac{\tan(\phi_V^{m,n})}{w\cdot\cos(\phi_H^{m,n})}\cdot\log_{10}\frac{1}{|R_V(\phi_V^{m,n})|^2}+\frac{\tan(\phi_H^{m,n})}{h\cdot\cos(\phi_V^{m,n})}\cdot\log_{10}\frac{1}{|R_H(\phi_H^{m,n})|^2}\right) \end{aligned} \quad (5)$$

where R_V and R_H are the reflection coefficients of the vertical and horizontal walls respectively. We approximated the reflection coefficients in this paper as follows: floor (tile) as 0.1574, wall (brick) as 0.2037, wall (dry concrete) as 0.3112 and ceiling (plasterboard) as 0.0743 [14]. The DS path loss model can be expressed as (6) and (7):

$$PL^{DS}(d)[\text{dB}] = \begin{cases} PL_1^{DS}(d)[\text{dB}], & \text{for } d \le d_{break} \\ PL_2^{DS}(d)[\text{dB}], & \text{for } d \ge d_{break} \end{cases} \quad (6)$$

where

$$PL_1^{DS}(d)[\text{dB}] = PL_{FS}(d_\circ) + 10\times n_1\times\log_{10}\left(\frac{d}{d_\circ}\right)+L_{m,n_1}(d), \quad (7)$$

$$PL_2^{DS}(d)[\text{dB}] = PL_{break} + 10\times n_2\times\log_{10}\left(\frac{d}{d_{break}}\right)+L_{m,n_2}(d) \quad (8)$$

and

$$PL_{break}[\text{dB}] = PL_{FS}(d_\circ) + 10 \times n_1 \times \log_{10}\left(\frac{d_{break}}{d_\circ}\right)$$

Therefore

$$PL^{DS}(d)[\text{dB}] = PL_1^{DS}(d)[\text{dB}] + PL_2^{DS}(d)[\text{dB}] + X_\sigma^{DS} \quad \text{for } d \geq d_\circ,\ d_\circ = 1\,\text{m} \tag{9}$$

where $PL^{DS}(d)[\text{dB}]$ is the path loss at any distance d between Tx and Rx, $PL_1^{DS}(d)[\text{dB}]$ and $PL_2^{DS}(d)[\text{dB}]$ are the path losses before and after break point respectively, d_{break} is the break point while $PL_{break}[\text{dB}]$ is the path loss at break point. Additionally, X_σ^{DS} is a zero mean Gaussian random variable with standard deviation σ in dB, $L_{m,n_1}(d)$ and $L_{m,n_2}(d)$ are modal attenuations before and after the break point respectively.

DS path loss model is found by determination of the path loss exponent (PLE) n_1 (before break point) and n_2 (after break point) via the minimum mean square error (MMSE) method to minimize σ by simultaneously solving for n_1 and n_2 [8].

6. CLOSE-IN REFERENCE DISTANCE PATH LOSS MODEL

Single-slope CI path loss model can be expressed as:

$$PL^{CI}(d)[\text{dB}] = PL_{FS}(d_\circ) + 10 \times n_1 \times \log_{10}\left(\frac{d}{d_\circ}\right) + X_\sigma^{CI} \quad \text{for } d \geq d_\circ,\ d_\circ = 1\,\text{m} \tag{10}$$

where X_σ^{CI} is a zero mean Gaussian random variable with standard deviation σ in dB. $PL_{FS}(d_\circ) = 10\log_{10}(\frac{4\pi d_\circ}{\lambda})$ at physically based reference distance $d_\circ$. The path loss model is found by determination of PLE, n_1 via minimum mean square error method [15].

7. DISCUSSION

The omnidirectional received power validated by the synthesized omnidirectional antenna pattern was used to model path loss in an indoor corridor at 18 GHz. The applied DS path loss model considers modal attenuation. The modal attenuation factor was determined following the structural design of the indoor corridor. The DS model was compared with CI model. The 18 GHz measurements was used in the validation and comparison of the two models. The measurements campaign was conducted at different Tx antenna heights (i.e., at 1.6 m and 2.3 m), and Rx antenna height fixed at 1.6 m for each of the Tx antenna heights.

Table 1 provides the best of fit PLE for the omnidirectional path loss analysis. The standard deviation for DS model in both Tx antenna heights are less than CI path loss model. The DS

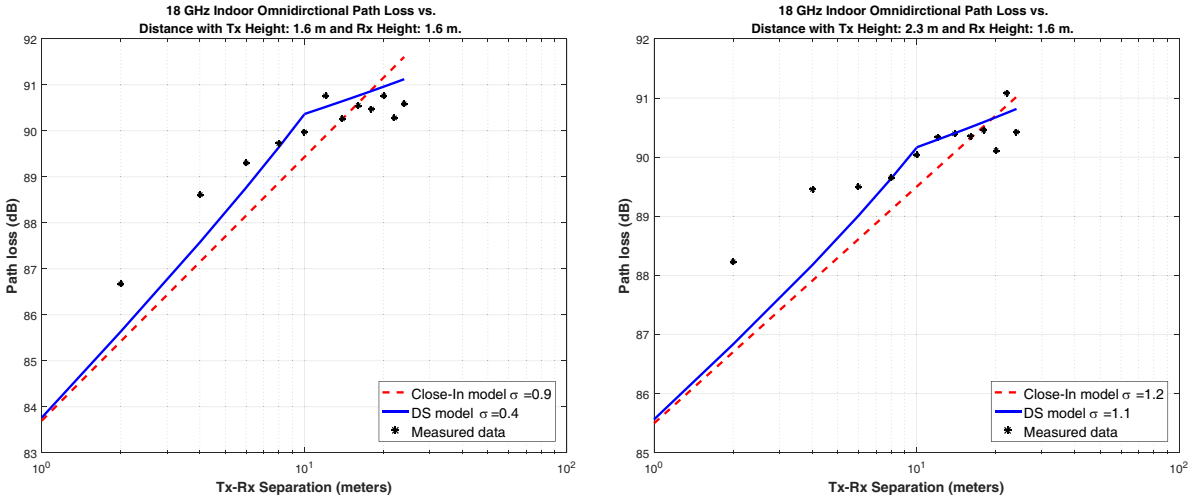

(a) (b)

Figure 4: 18 GHz single frequency omnidirectional large-scale path loss models with Rx antenna height fixed at 1.6 m and Tx antenna height at 1.6 m and 2.3 m above the floor. (a) Tx height: 1.6 m and Rx height: 1.6 m above the floor. (b) Tx height: 2.3 m and Rx height: 1.6 m above the floor.

Table 1: 18 GHz single frequency omnidirectional large-scale path loss parameters for DS and CI models with Rx antenna height fixed at 1.6 m and Tx antenna height at 1.6 m and 2.3 m above the floor.

Tx Height (m)	**Rx Height (m)**	**Path Loss Model**	**LOS**		
			PLE		
			n_1	n_2	σ[dB]
1.6	1.6	Close-In	0.6	-	0.9
		Dual Slope	0.6	0.2	0.4
2.3	1.6	Close-In	0.4	-	1.2
		Dual Slope	0.4	1.5	1.1

Table 2: LOS probability models as a function of distance d [m].

Model	**Description**
ITU-R	$P_{LOS} = \begin{cases} 1, & d \le d_{1\_1} \\ \exp\left(\frac{(-d(d-d_{1\_1}))}{a_1}\right), & d_{1\_1} < d < d_{1\_3} \\ b_1, & d \ge d_{1\_3} \end{cases}$
WINNER II (A1)	$P_{LOS} = \begin{cases} 1, & d \le d_{2\_1} \\ 1 - x_2(1 - (y_2 - z_2 \log_{10}(d))^3)^{\frac{1}{3}}, & d > d_{2\_1} \end{cases}$
Proposed	$P_{LOS} = \begin{cases} 1, & d \le d_{3\_1} \\ 1 - x_3(1 - (y_3 - z_3 \log_{10}(d))^3)^{\frac{1}{3}}, & d_{3\_1} < d < d_{3\_2} \\ \exp\left(\frac{(-d(d-d_{3\_2}))}{c_3}\right) \cdot e_3, & d \ge d_{3\_2} \end{cases}$

Table 3: Parameters optimization.

Model	**Results**	**MSE**
ITU-R	$P_{LOS} = \begin{cases} 1, & d \le 1 \\ \exp\left(\frac{(-d(d-1))}{5}\right), & 1 < d < 3 \\ 0.72, & d \ge 3 \end{cases}$	0.0176
WINNER II (A1)	$P_{LOS} = \begin{cases} 1, & d \le 1 \\ 1 - 1.6(1 - (1 - 0.002 \cdot \log_{10}(d))^3)^{\frac{1}{3}}, & d > 1 \end{cases}$	0.0121
Proposed	$P_{LOS} = \begin{cases} 1, & d \le 1 \\ 1 - 1.6(1 - (1 - 0.002 \cdot \log_{10}(d))^3)^{\frac{1}{3}}, & 1 < d < 12 \\ \exp\left(\frac{(-d(d-12))}{6000}\right) \cdot 0.72, & d \ge 12 \end{cases}$	0.0081

model becomes a better path loss prediction model for 5G network deployment in indoor corridors. Evidently, the PLE drops by 4 dB per decade of distance for DS model after break point while CI remains constant at 6 dB per decade for the entire distance along the corridor. In Fig. 4, a break point is established at approximately 12 m from the transmitter [8].

The MMSE was used as the technique for optimal parametrization of LOS probability models. The 18 GHz indoor corridor measurement data and the evaluated results are shown in Fig. 5. The validation results are summarized in Table 3. The proposed model fits the propagation data in indoor corridor better than other three existing indoor hotspot models as shown in Table 3.

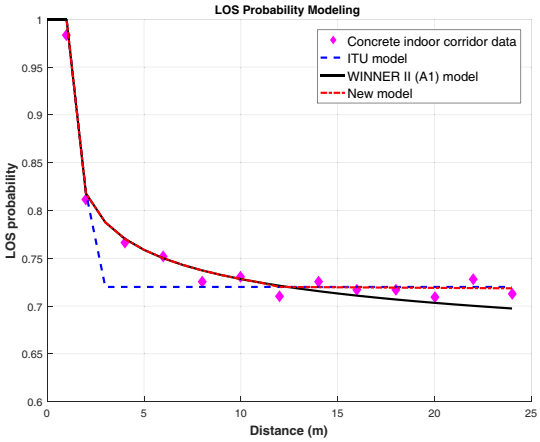

Figure 5: LOS probability vs distance.

8. CONCLUSION

This paper presents synthesis of omnidiectional path loss model at 18 GHz in indoor environment. Horn antenna radiation pattern has been used to validate the omnidirectional path loss synthesis. Accordingly, two path loss models i.e., DS and CI models are fitted into the measured data. The DS model is observed to have better performance in indoor corridors as compared to CI model as shown in Table 1. Omnidirectional path loss is important in 5G system design as engineers can use any antenna with arbitrary radiation pattern for network deployment.

LOS probability models are presented.The proposed model is seen to have out performed the International Telecommunication Union Recommendation (ITU-R) and WINNER II (A1) models. The LOS probability is essential for establishment of the network coverage capability. For indoor applications, a new model is proposed with an error margin of 0.81% as compared to ITU-R and WINNER II (A1) models with error margins of 1.76% and 1.21% respectively.

REFERENCES

1. Al-samman, A. M., T. A. Rahman, and M. H. I Azmi, "Indoor corridor wideband radio propagation measurements and channel models for 5G millimeter wave wireless communications at 19 GHz, 28 GHz, and 38 GHz bands," *Wireless Communications and Mobile Computing*, Vol. 2018, Mar. 2018, doi:10.1155/2018/6369517.
2. Rappaport, T. S., G. R. MacCartney, M. K. Samimi, and S. Sun, "Wideband millimeter-wave propagation measurements and channel models for future wireless communication system design," *IEEE Transactions on Communications*, Vol. 63, No. 9, 3029–3056, Sep. 2015, doi: 10.1109/TCOMM.2015.2434384.
3. Shu, S., G. R. MacCartney, M. K. Samimi, and T. S. Rappaport, "Synthesizing omnidirectional antenna patterns, received power and path loss from directional antennas for 5g millimeter-wave communications," *2015 IEEE Global Communications Conference (Globecom)*, Dec. 2015.
4. Rappaport, T. S., et al., "Millimeter wave mobile communications for 5G cellular: It will work!," *IEEE Access*, Vol. 1, 335–349, 2013, doi: 10.1109/ACCESS.2013.2260813.
5. Zhou, H., "Phased array for millimeter-wave mobile handset," *2014 IEEE Antennas and Propagation Society International Symposium (APSURSI)*, 933–934, Jul. 2014.
6. MacCartney, Jr., G. R. and T. S. Rappaport, "73 GHz millimeter wave propagation measurements for outdoor urban mobile and backhaul communications in New York City," *2014 IEEE International Conference on Communications (ICC)*, 4862–4867, Jun. 2014.
7. Hur, S., et al., "Synchronous channel sounder using horn antenna and indoor measurements on 28 GHz," *2014 IEEE International Black Sea Conference on Communications and Networking (BlackSeaCom)*, 83–87, May 2014.
8. Oyie, N. O. and T. J. O. Afullo, "Measurements and analysis of large-scale path loss model at 14 and 22 GHz in indoor corridor," *IEEE Access*, Vol. 6, 17205-17214, 2018, doi: 10.1109/ACCESS.2018.2802038.
9. WINNER II D 1.1.2, "WINNER II channel models, part II, Radio channel measurement and analysis results," Sep. 2007.

10. Report ITU-R M.2135-1, "Guidelines for evaluation of radio interface technologies for IMT-Advanced," Dec. 2009.
11. 3GPP TR 36.873, "Study on 3D channel model for LTE," Jul. 2015.
12. "Far field radiation from electric current," [Online]. Available: http://www.thefouriertransform.com/applications/radiation.php.
13. Fushini, F. and G. Falciasecca, "A mixed rays-modes approach to the propagation in real road and railway tunnels," *IEEE Transactions on Antennas and Propagation*, Vol. 60, No. 2, 1095–1105, Feb. 2012.
14. Sato, K., et al., "Measurements of reflection characteristics and refractive indices of interior construction materials in millimeter-wave bands," *IEEE 45th Vehicular Technology Conference. Countdown to the Wireless Twenty-First Century*, Vol. 1, 449–453, Chicago, IL, 1995, 10.1109/VETEC.1995.504907.
15. McCartney, G., T. S. Rappaport, S. Sun, and S. Deng, "Indoor office wideband millimetre-wave propagation measurements and channel models at 28 and 73 GHz for ultra-dense 5G wireless networks," *IEEE Access*, Vol. 3, 2388–2424, Dec. 2015.